NASA TM X-1411

PERFORMANCE OF 10-KILOWATT-CARBON-ARC SOLAR RADIATION SIMULATOR

By Gary C. Goldman and Kenneth Yass

Lewis Research Center
Cleveland, Ohio

NATIONAL AERONAUTICS AND SPACE ADMINISTRATION

For sale by the Clearinghouse for Federal Scientific and Technical Information
Springfield, Virginia 22151 – CFSTI price $3.00

PERFORMANCE OF 10-KILOWATT-CARBON-ARC SOLAR RADIATION SIMULATOR

by Gary C. Goldman and Kenneth Yass

Lewis Research Center

SUMMARY

A commercially available 10-kilowatt-carbon-arc solar-radiation simulator was evaluated. The simulator used molded lenticular lenses to improve irradiance uniformity, and a nonconsumable tungsten negative electrode was used to provide long-term continuous operation. The following solar simulation parameters were measured: irradiance, uniformity of irradiance, spectral energy distribution, uniformity of spectral energy distribution, collimation, irradiance stability, and radiant efficiency.

INTRODUCTION

The value of a solar radiation simulator depends on its ability to reproduce the solar radiation found in space accurately. All simulators deviate to some extent from the sun's known characteristics and can be described by the following parameters; total irradiance, uniformity of total irradiance, spectral energy distribution, uniformity of spectral energy distribution, collimation angle, and irradiance stability. Lack of knowledge of these deviations can produce misinterpreted results and substantial errors in the type of environmental testing being carried out at the Lewis Research Center. Examples of such errors would be lower temperatures or heating rates measured in shadowed areas of a particular irradiated model as a result of the excessive collimation angle of the incident beam (ref. 1) or an erroneous absorptivity-emissivity ratio measurement of an irradiated surface due to a spectral mismatch (ref. 2).

The procedures and results obtained in evaluating the performance of a particular commercially available 10-kilowatt-carbon-arc solar radiation simulator are presented herein. This unit, a Strong Arcomatic Solar Radiation Simulator #75002-A, differs from others in its power range in employing a molded lenticular or mosaic lens optical system and a nonconsumable tungsten negative electrode (refs. 3 and 4). This electrode allows up to 100 hours of continuous operation.

DESCRIPTION OF SYSTEM

The solar simulator system is composed of an arc lamp and an on-axis optical system located in a housing to which is affixed a power supply. The lamp consists of a positive electrode assembly, a negative electrode assembly, and provisions for starting and maintaining the arc. The positive electrode (anode), a cored carbon rod with ends suitable for automatic joining during operation, is maintained at a constant arc length from the negative electrode (cathode). The cathode is a nonconsumable argon-bathed tungsten rod that replaces the conventional carbon negative electrode. The optical elements, shown schematically in figure 1, consist of an aluminized elliposidal mirror for collecting the arc radiation, a large-diameter molded lenticular lens and a smaller lenticular lens designed to improve the irradiance distribution at the target plane, an aperture, and a projection lens, which images the aperture at the target plane. Power for the arc lamp is furnished by a selenium rectifier direct-current supply. All cooling is integrated into the system, although the lamp housing must be vented to an external exhauster.

MEASUREMENT PROCEDURES

The system was operated according to the manufacturer's recommendations, and measurements of the solar simulation parameters were made. To measure irradiance and uniformity of irradiance, a remote-controlled circularly and radially positioning scanner was located at the target plane. One thermopile detector having approximately a 3-millimeter-diameter sensitive surface and a 0.5-second time constant was held stationary in the target plane at a preset reference point. This detector monitored the time variation of irradiance. A second detector having the same diameter and time constant was transported incrementally across a diameter of the target plane by the scanner to obtain a spatial variation of irradiance. At each stationary position, every 45° and every 0.05 meter of diameter, the output signal of the scanning detector, as well as that of the reference detector, was recorded. This procedure was repeated for two distances from the projection lens. Accuracies of these irradiance measurements were ±2 percent.

A filter radiometer with a set of 22 filters was used to determine the spectral energy distribution. Measurements were made on-axis in the target plane. Variation in the spectrum with respect to the position in the target plane was also investigated by employing the filter radiometer at three different locations in the plane. These results were then processed by a procedure developed at the Lewis Research Center by Wagoner and Pollack (ref. 5).

The total collimation angle was measured by determining the size of the apparent source (fig. 1) and the distance from the apparent source to the target plane.

Irradiance stability measurements, which were made for long-term drift as well as for short-term fluctuations, were obtained with a cadmium sulfide detector positioned in the target plane. Its time constant of 55 milliseconds permitted the detector to respond to rapid irradiance fluctuations. Measurements were made both between and during the electrode joint disturbances.

Radiant efficiency is the ratio of the power delivered to the target plane to the input power to the arc. This efficiency was calculated by integrating the power in the target plane, as obtained from the irradiance uniformity data, and dividing this target plane power by the arc input power.

RESULTS AND DISCUSSION

The irradiance profiles in solar constants (1400 W/m^2 = 1 solar constant) as a function of radial position for the horizontal diameter at both 6.09- and 5.49-meter distances from the projection lens are shown in figure 2. At the 6.09-meter distance, the maximum beam diameter was 1.02 meters, but only the area within a 0.66-meter-diameter circle exhibited an irradiance variation of less than ±5 percent. At the 5.49-meter distance, the maximum beam diameter was 0.92 meter with an area within a 0.56-meter-diameter circle having a variation of less than ±5 percent. The irradiance decrease along the optical axis between these two distances was 0.51 solar constants per meter.

The spectral energy distribution obtained from filter measurements is compared with the filter equivalent curve (ref. 5) of the Johnson extraterrestrial solar energy distribution (ref. 6) in figure 3. The areas under both curves are equal. The cumulative energy under the curves of figure 2 is presented in table I. The spectral energy distribution, as compared with the Johnson distribution, shows a deficiency of energy in the ultraviolet region and the visible (0.4 to 0.7 micron) region of approximately 35 and 20 percent, respectively, and an excess in the infrared portion of the spectrum of approximately 25 percent. The variation of spectrum as a function of position in the target plane is less than ±2 percent from 0.35 to 2.50 microns and ±50 percent from 0.25 to 0.35 micron. The variation of ±50 percent is due to difficulities in the low microvolt signal level.

The total collimation angle is 2.3° throughout the test plane at the 6.09-meter distance. The total collimation angle of the sun by comparison is about 0.5°.

Beam intensity fluctuations over a 1-minute interval were in the order of ±1 percent, as was the drift during the consumption of an entire electrode. The burning time for one anode is about 32 minutes with an arc disturbance caused by a burning joint lasting for about 3 minutes. Fluctuations during the burning of a joint were approximately ±5 percent.

At the 6.09-meter distance there were 730 watts over the entire 1.02-meter-diameter beam. With an arc input power of 10.7 kilowatts, the total radiant efficiency is approximately 7 percent. Over the ±5-percent portion of the target plane (0.66 m), there are 480 watts, which yields an efficiency of about 4.5 percent.

The deviations from the extraterrestrial sun exhibited by this solar simulator indicated that a prospective user of the simulator must decide whether it is suitable for his particular application. He should then determine what corrections will be necessary.

Lewis Research Center,
National Aeronautics and Space Administration,
Cleveland, Ohio, March 14, 1967,
124-09-05-03-22.

REFERENCES

1. Bobco, R. P.; and Ishimoto, T.: Temperature Errors in Simple Systems Caused by Deviations from Ideal Space-Solar Simulation. Proceedings of the International Symposium on Solar Radiation Simulation, Los Angeles, Jan. 18-20, 1965. Institute of Environmental Sciences, 1965, pp. 1-11.

2. Diedrich, James H.; and Curtis, Henry B.: Experimental Investigation of Total Emittance and Solar Absorptance of Several Coatings Between 300° and 575° K. NASA TN D-3381, 1966, p. 5.

3. Freeman, R. S.: Recent Engineering Developments in the Carbon Arc Solar Simulator. Proceedings of the International Symposium on Solar Radiation Simulation, Los Angeles, Jan. 18-20, 1965. Institute of Environmental Sciences, 1965, pp. 139-143.

4. Cedargren, J. T.; Harrington, R. E.; and Riek, M. R.: Recent Advances in the Adaptation of Carbon Arcs to Solar Simulation. Proceedings of the Space Simulation Testing Conference, Pasadena, Nov. 16-18, 1964. Publ. CP-11, AIAA, 1964, pp. 146-154.

5. Wagoner, Ralph E.; and Pollack, John L.: Data Reduction for Filter Spectroradiometry. NASA TN D-3037, 1965.

6. Johnson, Francis S.: The Solar Constant. J. Meteorology, vol. 11, no. 6, Dec. 1954, pp. 431-439.

TABLE I. - CUMULATIVE SPECTRAL ENERGY DISTRIBUTION OF SOLAR SIMULATOR AND EXTRATERRESTRIAL SOLAR CURVE

Wavelength, μm	Solar simulator, percent of total energy	Johnson, percent of total energy	Wavelength, μm	Solar simulator, percent of total energy	Johnson, percent of total energy
0.25	0.3	0	1.55	84.3	90.8
.30	.9	1.3	1.60	85.8	91.7
.35	2.4	4.6	1.65	87.2	92.4
.40	6.1	9.6	1.70	88.5	93.1
.45	10.9	16.0	1.75	89.6	93.8
.50	16.1	23.6	1.80	90.5	94.4
.55	21.8	30.9	1.85	91.4	94.9
.60	27.4	37.8	1.90	92.1	95.4
.65	32.6	44.1	1.95	92.9	95.8
.70	37.5	49.8	2.00	93.7	96.2
.75	41.8	54.8	2.05	94.5	96.6
.80	45.9	59.2	2.10	95.3	97.0
.85	49.9	63.1	2.15	96.0	97.3
.90	54.0	66.6	2.20	96.7	97.6
.95	57.7	69.8	2.25	97.4	98.0
1.00	60.8	72.6	2.30	97.9	98.2
1.05	63.7	75.2	2.35	98.7	98.5
1.10	66.6	77.5	2.40	98.8	98.8
1.15	69.4	79.7	2.45	99.2	99.0
1.20	72.0	81.6	2.50	99.5	99.2
1.25	74.2	83.4	2.55	99.7	99.3
1.30	75.9	84.9	2.60	99.9	99.5
1.35	77.4	86.3	2.65	100.0	99.6
1.40	79.0	87.6	2.70	100.0	99.8
1.45	80.8	88.8	2.75	100.0	99.8
1.50	82.6	89.9	2.80	100.0	99.9

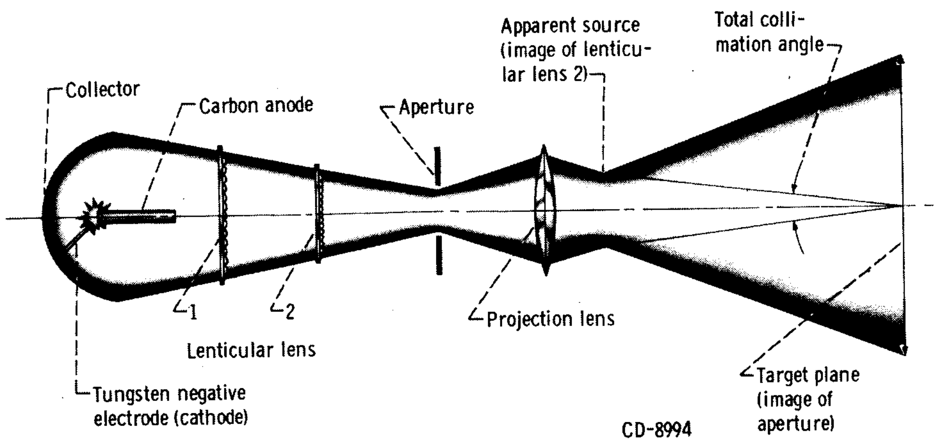

Figure 1. - Solar simulator optical elements.

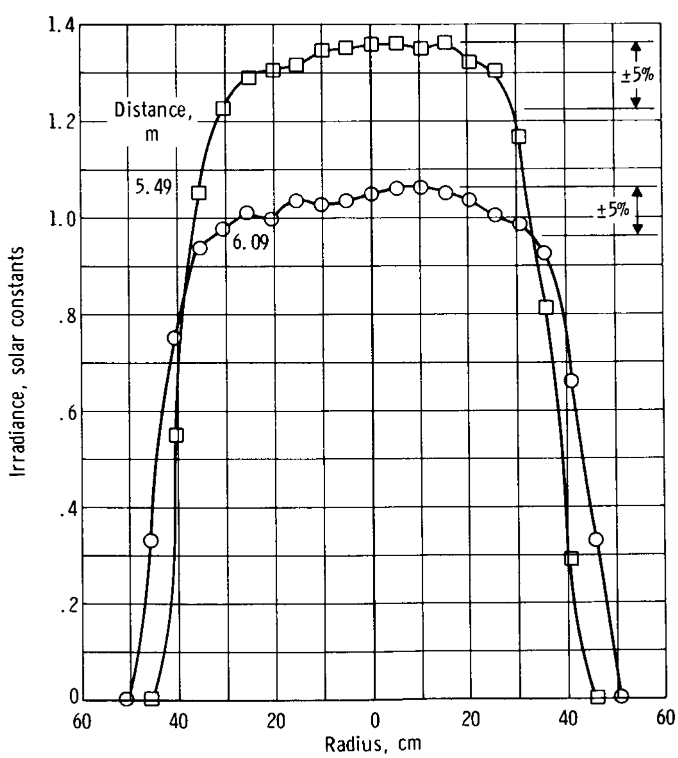

Figure 2. - Irradiance variations across horizontal diameter in target plane of 10-kilowatt-carbon-arc solar simulator at 5.49 and 6.09 meters from projection lens.

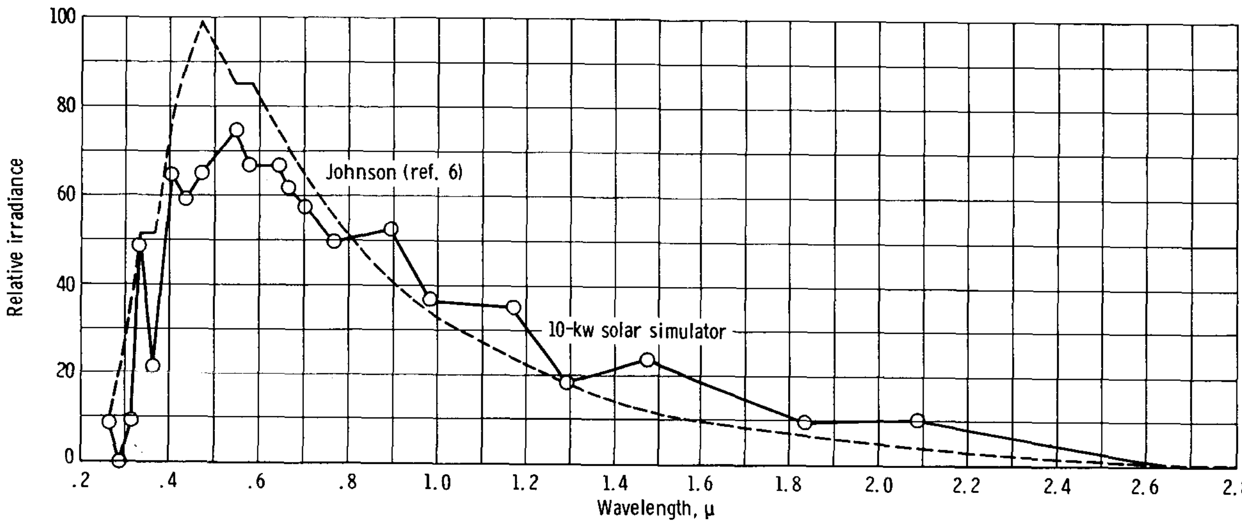

Figure 3. - Comparison of spectral energy distribution for 10-kilowatt-carbon-arc solar radiation simulator with that for Johnson's extraterrestrial solar curve.